JOURNAL OF NANO- AND ELECTRONIC PHYSICS
Vol. **5** No 4, 04019(3pp) (2013)

ЖУРНАЛ НАНО- ТА ЕЛЕКТРОННОЇ ФІЗИКИ
Том **5** № 4, 04019(3cc) (2013)

Short Communication

Mechanisms of Fractal Formation in Colloidal Carbon-Bearing Natural System

A.P. Kuzmenko[1], V.V. Chakov[2], Chan Nyein Aung[1], M.B. Dobromyslov[3]

[1] *Southwest State University, 94, 50 Let Oktyabrya Str., 305040 Kursk, Russia*
[2] *Institute of Water and Ecological Problems, FEB RAN, 65, Kim-Yu-Chen Str., 680063 Khabarovsk, Russia*
[3] *Pacific National University, 136, Tihookeanskaya Str., 680035 Khabarovsk, Russia*

(Received 24 November 2013; published online 10 December 2013)

By using the advanced nano-approach processes and phenomena in self-organizing colloidal systems are studied. The conditions of appearance of self-organized phenomena are determined and also ranges of operation of diffusion, capillary, and fractalization mechanisms are found.

Keywords: Self-organization, Colloidal system, Fractal and nano-sized structures, Capillary and diffusion phenomena.

PACS numbers: 05.65. + b, 61.43. Hv

1. INTRODUCTION

An increasingly growing interest in the capability of nano-sized entities to self-organization and designing, on this basis, practically important devices is well understood and, for the most part, dictated by successes in nanoelectronics [1]. To implement the processes of self-assemblage at nano-level requires finding effective driving parameters that must be, obviously, associated with the size and structure of micro- and nanoparticles in space-organized systems [2, 3] including external gradient fields [4, 5].

2. EXPERIMENTAL RESULTS AND DISCATIONS

The object of the paper was to study sizes, chemical structure, and elemental distribution of self-organized entities in micro- and nanosystem region formed from colloidal carbon-bearing specimen, features and regularities of the formation on solid-phase surfaces.

Samples from natural doped carbon-bearing peat have a set of properties (the capability to microphase stratification, the existence of heterogeneous and heterophase micro- and nano-structure and others) that add to the study of mechanisms of fractal formation on nano-scale level. The samples were prepared in conditions limited in diffusion (the drop deposition method) at which: $E_b > E_{inter} \geq E_{kin} > E_d$, that is the bonding energy of particles with a substrate (E_b) was greater than the intermolecular interaction energy (E_{inter}), kinetic (E_{kin}), and also the energy of their diffusion (E_d). This condition is supported by the estimation of values of relevant energies with consideration for given in Fig. 1a their confocal microscopic (CM) (Omega Scope, AIST-NT) images at magnifications of 505 $^{\times}$ to 2830 $^{\times}$ shows microstructure formation at the drop's edge after drying. Fig.1b gives electron-microscopic (SEM) image of structures within the central region, Fig. 1c – atomic force (Smart SPM AIST-NT) microscopic (AFM) image of structures in the intermediate region, namely, between the edge and the center.

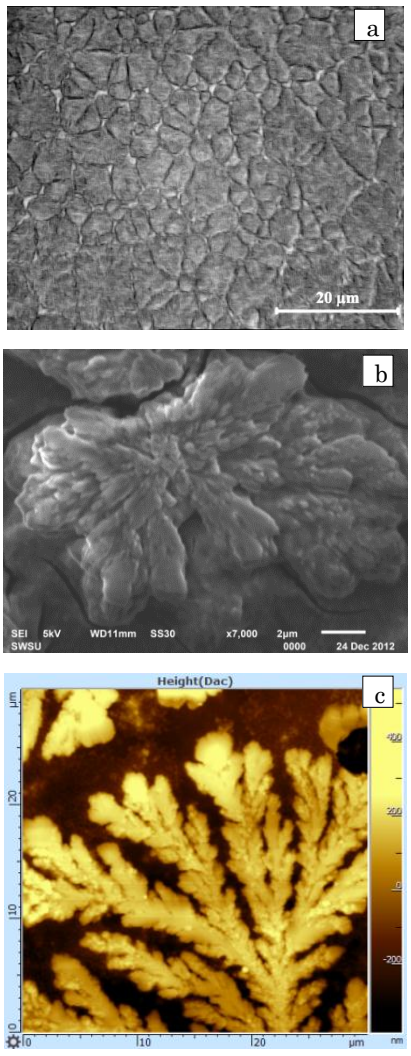

Fig. 1 – Images of structural formations: a – KM at the edge at 2830 $^{\times}$; b – SEM in the central part at 7000 $^{\times}$; c – AFM image of the part of the fractal

The distribution of chemical elements in regions given in Fig. 1a-c obtained with scan electron microscope (SEM) with energy dispersive adapter (EDA)

The article was reported at the International Conference «Physics and Technology of Nanomaterials and Structures», Kursk, 21-22 November, 2013

(JEOLJSM6610LV, EDX Oxford Instruments) is shown in Fig. 2. From all metals found by EDA technique - Na, Si, Cu, K, Ca, Fe, Zn, Mn in fractal branches (Fig. 1c) Al (27 %) had the maximum content. Whereas it's content in fractal center was 9-fold lower, and at the drop's edge was lower than 1 %. Among all found metals Al had the maximum content. Also, alumosilicate phases in organic carbon formations were found to be present in dominant contents. According to X-ray phase analysis (XRD) data (GBC EMMA, CuK_α) a clear-cut line 3.32 Å corresponding to $Al_2O_3 \times 2SiO_2 \times 2H_2O$ appeared. All other metals listed were found to be equal in content in all regions studied and was not greater than 1 %. According to XRD data identified were the compounds of the type: $MgSO_4$, $CaSO_4 \times nH_2O$, $SiO_2 \times nH_2O$, $CaO \times SiO_2 \times H_2O$, $CaO \times Fe_2O_3 \times 6H_2O$ and other hydrates and oxides. Carbon was dominated in all sample's regions, which, in essence, is responsible for all physico-chemical properties of studied peats.

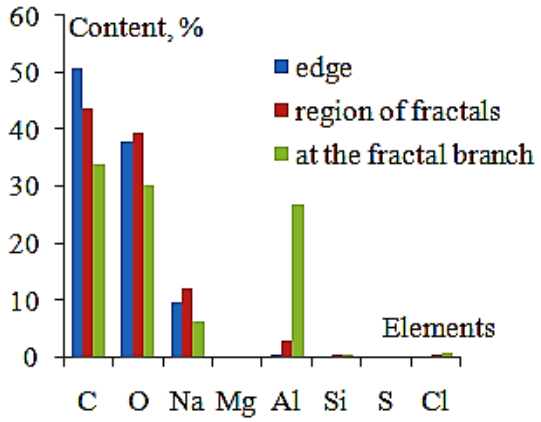

Fig. 2 – Distribution of chemical elements in various parts of the sample

In line with earlier data [3, 4] the condition $E_b > E_{inter} \geq E_{kin} > E_d$ must be supplemented with the maximum energy of the surface tension E_s, which corresponds to nano-size of structural components that form the fractal branches starting from 5 nm according to data of AFM, SEM, and small-angle X-ray scattering (SAXSeesmc², Anton Paar): $E_s > E_b > E_{inter} \geq E_{kin} > E_d$.

This inference is in line with the results of Raman Scattering (RS) and fluorescent microscope (FM) obtained with microspectrometer, which was integrated with AFM, by mapping technique (Fig. 3a-d) at excitation on $\lambda = 473$ nm. It is seen a dramatic difference between FM and RS mapped images: (Fig. 3a) is characterized by finer micro- and nanostructure even compared to AFM image in an equal scan field – 30 × 30 μm (Fig. 1c). Comparison of FM and RS images indicates that fractal branches were formed by nano-particles of significantly lower size. Comparison of intensity of RS lines by the base and at branches, according to RS images on line 1420 nm (Fig. 3b), is indicative of its reduction by several-fold along with broadening. It is in this region that the reduction of particle size takes place with consideration for the Heisenberg uncertainty principle $\Delta E \Delta t = \hbar$. The same result was found earlier [4] from comparison of rotational oscillations amplitudes (See Fig. 3 [4]) in different points (at the branch and stem) of fractals. So the lines in RS spectra become wider and their intensity decreases and shift to low-frequency region appears.

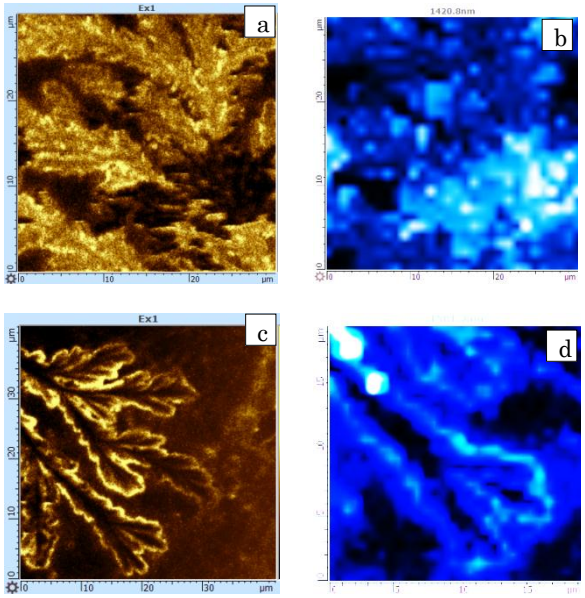

Fig. 3 – Mapped images of fractal branches according to data of FM and RS for an initial (a and b) and photoactivated with H_2O_2 peat sample (c and d)

The photoactivation of peat colloidal system conducted with diluted to 3 % H_2O_2 made it possible to obtain more contrast images of fractal branches both in FM and RS. Further concentration increase led to the decomposition of metal-bearing mineral inclusions and made FM image poorer. The increase in intensity of RS and FM at external parts of branches was possibly due to carrying out into these regions of larger nano-particles after processing with H_2O_2. Comparison of elemental distribution data (Fig. 2) with RS and FM mapped images suggests that nano-particles of metal oxides (Al_2O_3 and oxides of other transitional metals in dramatically lower contents) may be accumulated at external parts of fractal branches. The enhancement of FM contrast may be due to interband transitions at radiative recombination of excited electrons in d band. This is also attested by the absence a reasonable structural contrast at excitation of $\lambda = 352$ nm and its complete absence at $\lambda = 785$ nm, corresponding to lower quantum excitation energy. Seen in Fig. 3a, b abrupt change in contrast of FM and RS images (from black to the most bright by the basis of fractal) indicates dramatically greater sizes of nano-particles in this region. Correlation of RS and FM images with elemental distribution in various parts of fractal formations is inversely dependent on atomic mass: ~ $1/\mu$.

Forces acting when structuration of colloidal system from a drop takes place are the following: capillary, of diffusion, of internal friction, of interphase interaction and Van-der-Waals forces (the Lenard-Jones potential ~ 0.1 eV). Then the equation describing the drop surface may be written in the form: $y = h_0 - kT - vt$. Here h_0 is the maximum drop's thickness, $k = \text{tg}\ \alpha$, α is the inclination angle of the wedge "air-liquid-substrate", v is the velocity of the liquid free surface shift.

To consider diffusion and evaporation processes in this system as basic ones. To determine the dominant mechanism that brings about transition of colloidal particles to the drop's edges with consideration for its surface equation y according to [2] calculate the dimensionless parameter: $d = k^2DR / (h_0)^2$. To evaluate d consider that the diffusion component depends on the drop radius (transition of nano-particles from the center to edges $R = 3$ mm), the value of the angle α at the drop edge measuring several degrees ($k = \text{tg}\ \alpha < 0.1$ and the diffusion coefficient D was taken for water (2.4×10^{-9} m²/s) and water solution of a carbon compound (1.02×10^{-9} m²/s). Denominator is determined by evaporation whose value is dependent on the velocity of motion of the liquid edge to the center at evaporation: $v = L/t$, where L is drop diameter, t is evaporation time, $h_0 = 0.5$ mm. In this case the value of d turns out to be significantly lower than 1, supporting the possible formation of structures at the drop edge due to the diffusion mechanism. Following the same procedure one can obtain and the conditions of structure formation in other regions: at the fractal – due to capillary, and at the fractal branches – fractalization mechanisms, when $d = 1$ и $d > 1$, respectively.

The role of capillary mechanism can be evaluated by the value of the Bond number that is equal to the ratio of Rayleigh's and Marangoni's numbers: $K_B = \rho g \chi h_0^4 / \sigma$. Here g is gravitational acceleration, ρ is water density, χ temperature conductivity, h_0 is the layer thickness and σ is surface tension of the medium. Let us consider water as the basic medium and take ρ and χ for it. Take into consideration that fractals begin form at the last stage of evaporation, when the incoming energy is maximal and the colloidal system turns dramatically non-equilibrium.

Then h_0 becomes comparable with nano-particles sizes $h_0 = d \sim 5 \div 70$ nm, and the value of σ highly grows: $\sigma = E_s / S$, since $S = \pi d^2$ for nano-particles decreases and surface energy increases. Under these conditions K_B becomes considerably lower than 1, corresponding dominant in this region capillary forces that are responsible for the fractal formation.

For the appearance of self-organization non-equilibrium is needed which in the present method (wedge-like dehydration) is afforded by only evaporation. Equation of motion of colloidal particles is determined in terms of the resultant of all forces: $mdx/dt = \Sigma F_i$, whose solution must describe the distribution of particles. However, the existence of many parameters (viscosity, surface tension, etc.) that determine the forces hampers the solution of dynamical problem. To analyze the interaction in the studied mixed organic and inorganic system, following [1], consider potential energy that includes both physical and chemical sorption. The resulting dependence of interaction energy on the interparticle distance is characterized by two minima, namely, the first is due to covalent and ionic intra-atomic bonds, whereas the physical sorption occurs at interatomic distances greater than 0.3 nm. It is obviously that the boundary region (Fig. 1a) is formed due to chemical sorption, and the second minimum corresponds to the region of fractal formations (Fig. 1c) where nano-particles are structured having lesser size as shown earlier. The maximum of negative attraction energy corresponds to an unstable equilibration state. Nonetheless, this may lead to an association of particles of various sizes, which is objectively observed (Fig. 1b). Comparison of observed confocal and AFM images given in Fig. 1a-c considering inferences [2] makes it possible to associate their formation from the colloidal system with the following mechanisms: viscous – (Fig. 1a), capillary – (Fig. 1b), and fractalization – (Fig. 1c).

3. CONCLUSIONS

Thus, in nano-structural studies of natural colloidal systems the conditions of appearance of self-organized phenomena have been determined, and also ranges of operation of diffusion, capillary, and fractalization mechanisms have been found.

REFERENCES

1. A. Kuhnle, *Curr. Opinion Colloid & Interface Sci.* **14**, 157 (2009).
2. R. Holtzman, M.L. Szulczewski R. Juanes, *Phys. Rev. Lett.* **108**, 264504 (2012).
3. A.P. Kuzmenko, V.V. Chakov, N.A. Chan, P.V. Abakumov, D.I. Timakov, *Proceedings of the Southwest State University, Part 2* No 6 (39) (2011).
4. A.P. Kuzmenko, V.P. Dobritsa, Chan Nyein Aung, *Scientific Sheets of the Belgorod State University. Series Mathematics, Physics* No 11 (154), Issue 31 (2013).
5. Yu.Yu. Tarasevich, *Phys.-Usp.* **174** No 7 (2004).